Materials Physics and Mechanics 37 (2018) 109-117 Received: December 22, 2017

STUDY OF THE PROPERTIES OF CU-CONTAINING POLYACRYLONITRILE NANOSTRUCTURED GAS-SENSING FILMS

T.V. Semenistaya

Institute of Nanotechnologies, Electronics and Equipment Engineering, Southern Federal University,

2 Shevchenko Str., Taganrog, 347928, Russia

e-mail: semenistayatv@sfedu.ru

Abstract. The Cu-containing polyacrylonitrile (PAN) thin films (0.04 – 0.6 μm thicknesses) were fabricated using IR-pyrolysis in ambient argon in different temperature and time modes. The films were studied by X-ray photoelectron spectroscopy (XPS), X-ray diffraction (XRD), transmission electron microscopy (TEM) and atomic force microscopy (AFM). CuCl, Cu_2O and Cu crystalline inclusions were obtained in the nanocomposite films by XRD. The film microstructure was analyzed by AFM and TEM: the typical morphology corresponds to composite film with nanoparticles of 10 nm average size in the polymer matrix. The film electrical resistance was in the range from $4.0 \cdot 10^2$ to $2.7 \cdot 10^{11}$ Ω. The Cu-containing PAN nanocomposite films are promising for application as low-temperature NO_2 sensor in 36.5 – 255 ppm concentration range.

Keywords: IR-pyrolized polyacrylonitrile; electroconductive organic polymers; gas-sensing materials; nanostructured films; AFM; XPS; XRD; TEM.

1. Introduction

Polymeric materials have gained a wide theoretical interest and can be used for very different purposes and demonstrate unique possibilities [1 – 3]. Recent advances in polymer science and film preparation have made polymeric material films useful, practical and economical in a wide range of sensor designs and applications [4 – 12]. PAN is extremely popular and attracts much attention due to its unique structure. It is capable to change its microstructure under heating, possesses tolerance to most solvents and commercial availability [13 – 17]. Hydrolyzed PAN membranes widely used as a support for the assembly of a composite membrane and play an important role in the processes of pervaporation, bioproduct purification and water treatment [18]. PAN membranes, prepared via thermally induced phase separation process using dimethylsulfone/glycerol as the mixed diluents, may be suitable for micro- or ultra-filtration processes in water treatments [19]. The pyrolyzed PAN becomes conducting conjugative polymer matrix and acts as a buffer to relieve the morphological change of Sb, and as an inactive component to prevent the further aggregation of Sb during cycling. Nano Sb and Sn encapsulated pyrolytic PAN composites are used for anode material in lithium-ion batteries [20, 21].

The recent review by Nataraj et al. [22] describes the chemistry and applications of PAN-based nanofibers. PAN is the most commonly used polymer for producing carbon nanofibers, mainly due to its high carbon yield (up to 56%), flexibility of tailoring the structure of the final carbon nanofiber products due to the formation of a ladder structure via nitrile polymerization. The chemistry of PAN is of particular interest because of its use as a precursor in the formation of carbon nanofibers for different applications, including porous

http://dx.doi.org/10.18720/MPM.3722018_1

structured carbon nanofibers of high surface area for elecrtronics and energy storage applications [22]. Therefore, PAN-based nanofibers have been the subject of considerable interest, PAN nanocomposites, combined with various transition metal compounds, were found as better choice for gas-sensing material due to their good environmental and chemical stability, ease of synthesis, inexpensive monomer and their ability to change the structural and electric properties under thermal treatment. This inspires the idea that PAN films can be appropriate material for high performance sensors. PAN films can be considered as one of the most promising material in order to obtain chemo-resistive sensors for environmental applications.

In this paper, we describe low-cost flexible sensors, used for the detection of nitrogen dioxide and based on a conducting nanocomposite Cu-containing PAN films, obtained by IR-pyrolysis in ambient argon. The electrical transport properties of the fabricated films, deposited on polycor substrates were evaluated from electrical measurements, performed at different temperatures. Sensing measurements were performed under exposition to calibrated nitrogen dioxide gas at concentration ranging between 36.5 ppm and 255 ppm with air as the buffer gas, at different temperatures and under different relative humidity levels.

In the present work, we studied gas-sensing properties of the Cu-containing PAN nanocomposite films in dependence on a modifying additives concentrations and technological parameters of the films fabrication that influence the formed polymer structure.

2. Experimental technique

Thermally treated PAN polymer shows a rich evolution of structural and electric properties: the chains undergo cyclization to form a conjugated-chain chemical structure, resulting in electrical conductivity. PAN becomes a conjugated conducting polymer by low temperature pyrolysis [23, 24]. On the other hand, PAN is a very processable polymer, which can be dissolved in DMF. It is also found that the doping of PAN prior to carbonization can alter the physicochemical nature of the polymer under the thermal treatment [25]. The thermal treatment of PAN leads to changes in physical properties, which are of great practical importance. A perspective application of this thermal treatment of PAN was found, when this polymer was used as a precursor to produce high quality carbon materials. An early initiation and sufficient cyclization is an important precondition for obtaining stabilized carbon materials with uniform microstructure [26].

Fabrication of Cu-containing polyacrylonitrile films. The Cu-containing polyacrylonitrile films were fabricated by pyrolysis method under the influence of incoherent IR-radiation under inert atmosphere conditions. The following components were used: polyacrylonitrile (PAN) (Aldrich 181315) as a conductive polymer matrix, copper chloride (II) $CuCl_2$ as a modifying additive to increase the selectivity and adsorption activity of the nanocomposite films, dimethylformamide (DMF) as a solvent.

A film forming solution was prepared by dissolving 0.8 g PAN and copper chloride (II) in an amount of 0.2 – 10 wt. % in 20 ml DMFA under stirring at 90 ºC. After being cooled down to room temperature, the film-forming solution was deposited (centrifuged) on quartz substrates and then dried at 90 ºC for 30 minutes. Further, the samples were stored in air for 24 hours at 22 °C until full bleaching to extract the solvent.

IR-pyrolysis of the samples was carried out in several steps: the chamber of IR-radiation in ambient air was used at the first stage for oxidizing thermal stabilization of the PAN polymer; the IR-annealing device «Foton» was used in ambient argon at the second stage for PAN carbonization. Halogen lamps KG-220 with high radiation in the area of 0.8 μm – 1.2 μm were used as the source of radiation. Uniform heating of the samples was supplied with up and down position of the halogen lamps in the black lead cassette. The

thermoelectric couple chromium-aluminum inside the black lead cassette was used to control the intensity of IR-radiation. The temperature measurement accuracy was 0.25 ºC [27].

The time-temperature modes of IR-annealing were selected experimentally, since the intensity and duration of infrared radiation provide an opportunity to control the properties of the material films by changing the molecular structure of the polymer. The radiation intensity at the first stage of IR-annealing corresponds to temperatures of 150 ºC and 220 °C during a 15-minute period each sequentially, and the intensity of radiation at the second stage of the IR-annealing corresponds to temperatures of 500 – 800 °C during a 5 – 15-minute period [28].

Methods of film analysis. The thickness of the films was measured by the interferential microscopy using interferometer MII-4. The films structure was analyzed by X-ray diffraction (XRD) technique using DRON-6 with CuKα 1.54051 Å radiation. EFTEM (energy-filtered TEM) microanalysis was done using LEO 912 ABOMEGA transmission electron microscope fitted with an in-column Omega energy filter, having such characteristic as an operating accelerating voltage of 100 kV; magnification: 80 – 500000x; image resolution: 0.2 – 0.34 nm. The surface morphology was observed by atomic force microscopy (AFM) using scanning probe microscope Solver P-47. The X-ray photoelectron spectra were recorded by means of a Kratos Axis Ultra spectrometer using excitation with monochromatic Al Kα radiation (1486.6 eV). The residual pressure in the spectrometer during the experiments was $5 \cdot 10^{-7}$ Pa. The spectra were processed with the Vision 2 software package (Kratos Analytical). The accuracy of the binding energies (E_b) determination was ~ 0.1 eV, and that of the quantitative analysis was 10 rel. %. The binding energy scale was calibrated against the C1s line of aliphatic carbon (E_b = 285.0 eV). The specific resistance measurements were carried out using a source measure unit VIK-UES 07 by four-point probe method. The electrical characteristics of the prepared samples were carried out in a setup, equipped with heating element [29]. Ag contacts were deposited on the film surface using the electro conductive glue in order to investigate the electrical properties of the samples.

The steady-state gas distribution method was used for testing gas-sensing properties. A specially made setup, equipped with a quartz chamber, sensor holder, gas and purge lines, was used to maintain the desired level of detected gas concentration. Sensing characteristics were examined on base of the measurement of the film resistance. The quartz chamber volume was around 700 cm^3 so that the change in gas concentration was immediate and measurements of the response time and the recovery time of the sensors were accurate. The response time was defined as the time, required to achieve 90% of the total resistance change, when the detected gas is introduced into air. The recovery time is the time, required to achieve 90% of the total resistance change, when the detected gas admission is turned off and the air is reintroduced into the chamber. The gas sensitivity (S) was defined as the following ratio: $S = (R_0 - R_g)/R_0$, when $R_0 > R_g$, where R_0 is the resistance in air, R_g is the resistance in the atmosphere of the detected gas [30].

3. Results and discussion

PAN has a number of advantageous properties: (i) the solubility in polar solvents (DMFA, dimethylsulfoxide, dimethylacetatamide) turning into gel that is advantage for copper particles uniform distribution in the polymer organic matrix; (ii) the ability to form thin films; (iii) the change of electrophysical properties from dielectric to semiconducting material under IR-annealing [31].

The thickness of the prepared films was measured by the method of the interferential microscopy (Fig. 1). The films growth was observed in accordance with the technological parameters and different weight concentration of a modifying additive in film-forming solutions. The PAN films thickness was between 0.01 – 0.03 μm. The Cu-containing PAN films were of various thicknesses in the range from 0.04 to 0.6 μm.

The phase formation and the surface crystallization were analyzed by the XRD. There are CuCl, Cu_2O and Cu crystalline inclusions in the composites films (Table 1). The XRD pattern of the synthesized sample contains peaks that characterize crystalline inclusions in the samples. This result is in good agreement with the other XRD reports (Table 1) [32 – 34].

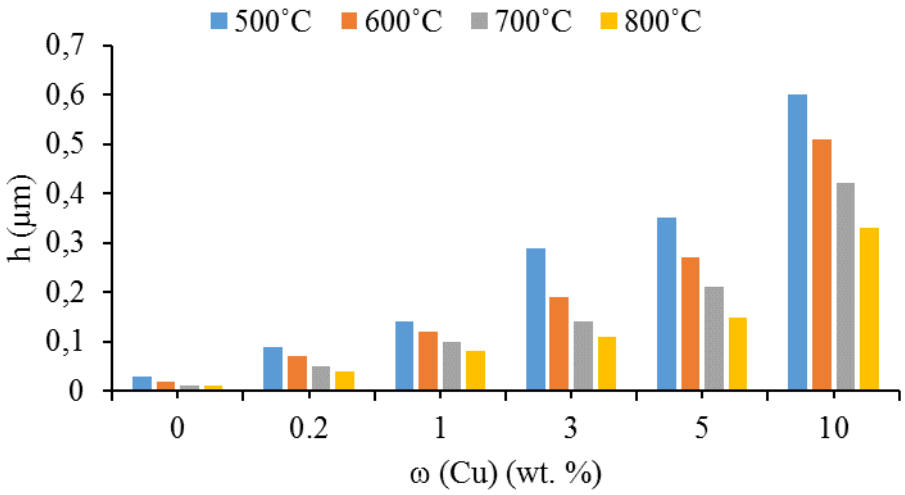

Fig. 1. 3D histogram, showing the films thickness dependence on the weight concentration of modifying additive and IR-pyrolysis temperature.

Table 1. XRD-data of the Cu-containing PAN films.

2θ					
CuCl		Cu_2O		Cu	
Tabular data	Actual data	Tabular data	Actual data	Tabular data	Actual data
28.12	28.22	37.01	37.05	43.29	43.36
36.42	36.02	–	–	–	43.6

The microstructure of the Cu-containing PAN film has been obtained, using EFTEM [35]. The micrograph clearly indicates copper compounds nanoparticles and their distribution, which size is 10 nm in average. We consider the polymer matrix stabilizes the nanoparticles and prevents their aggregation. The diffraction pattern indicates the crystalline order regardless of the light-sized nanoparticles. These TEM results were verified by XRD analysis [35].

X-ray photoelectron spectroscopy was used to study the composition and structural organization of the Cu-containing conducting polymer formed [36 – 39]. XPS survey and narrow scan data were taken on the film samples [35]. XPS survey spectra, acquired for the Cu-containing PAN film, are present in [35]. The peaks located at about 933 eV, 531 eV, 400 eV, and 285 eV correspond to the electron states of Cu2p, O1s, N1s and C1s in the PAN molecule, respectively. PAN, subjected to carbonization under controlled conditions, as it is known to transform into polymer with conjugated bonds [13, 16, 17, 24]. XPS signal characteristics of C1s, O1s, N1s confirm the well-known chemical structure of PAN polymer [35 – 41]. The C1s signal is dominated by a major peak at BE of approximately 284.7 eV. This peak can be attributed to aliphatic carbon (C – C) of the polymer chain, i.e. the carbon atoms bonded with carbon and hydrogen atoms [35, 36]. The intensity of the C1s peaks at 285.9 eV and at 286.7 eV, indicating the formation of carbon nitrogen atoms links in $(–CH_2CH(CN)–)_n$ and of imino bonds (C=N–) [35, 36, 44], respectively, is roughly equal.

The N1s core is on level spectrum of the Cu-containing PAN films. The large peak with its maximum at 398.4 is attributable to the imino-like (=N–) nitrogen atoms [45]. The peak at 400.4 eV can be seen due to carbons, linked to the nitrogen atom. The peak, located at 400.4 eV in the N1s core region corresponds to the binding energy of the nitrogen atoms in C–N=C bonds [45]. The peak-fit of the O1s core level reveals two binding energy states. The low-binding energy component at 530.9 eV is from CuO or Cu_2O. The high-binding energy component at 532,3 eV arises from carbon species, combined with oxygen (C=O, C–O–C) [43, 46].Two components by peak fitting the Cu XPS data were identified. The larger and narrower low-binding energy component at 932.6 eV is from metallic Cu or Cu(I) species and the higher binding energy component at 934.8 eV can be assigned to oxidized Cu [42 – 45]. In Table 2, the XPS elemental surface compositions of the Cu-containing PAN films are presented.

Table 2. Assignments of the main spectral bands, based on their binding energies (BE) and atomic concentration (AC) of the Cu-containing PAN films.

Element	BE (eV)	AC (at. %)	Assignments
C1s	284.7	81.1	$–(CH_2)–$
	285.9		$C≡N$ $(–CH_2CH(CN)–)_n$
	286.7		C–N, C=N, $(–CH_2CH(CN)–)_n$
	288.2		C=O, O–C–O
N1s	398.4	11.7	C=N–H
	400.4		–NH–, C–N=C
O1s	530.9	6.4	CuO, Cu_2O
	532.3		C=O, O–C–O
Cu2p	932.5	0.7	Cu^0, Cu^{1+} (Cu_2O)
	934.8		Cu^{2+} (CuO)

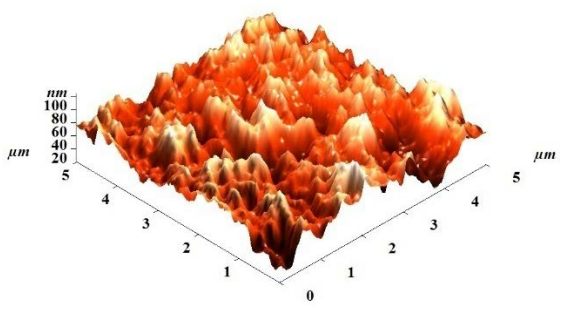

(a)

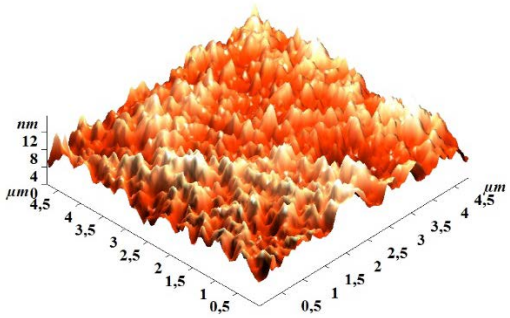

(b)

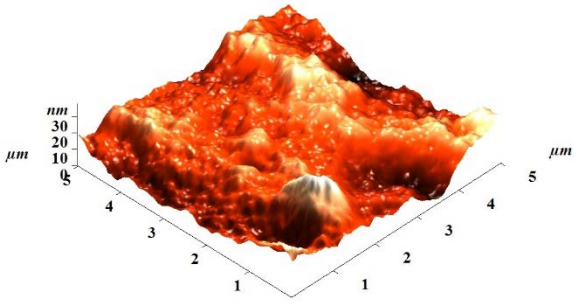

(c)

Fig. 2. AFM-images of the Cu-containing PAN films: 600-3 (a), 700-3 (b), 800-3 (c).

In order to observe clearly the microtopographical changes on the nanocomposite film surfaces, the AFM images of the film surfaces, formed under various time-temperature IR-annealing modes from film-forming solutions with different weight concentration of copper chloride (II), were taken and are shown in Fig. 2. It could be observed that the Cu-containing PAN films are dense and show a rough surface. When the IR-annealing temperature was increased to 800 ºC, a decrease in surface roughness was observed and the distribution of crystallite was uniform. High temperature enhances the crystallite size and the roughness decrease [42].

The statistical parameters of the surface morphology were estimated, using the Image Analysis software. Fig. 2 shows that the Cu-containing PAN samples change the surface roughness of the films due to fabrication temperature growth. It was noted that the surfaces became smoother. For example, the root-mean-square (*Rq*) surface roughness over an area of 5×5 μm^2 for the films changes from 15.4 nm to 1.9 nm, while forming films at 600 ºC and 700 °C, respectively [47].

Thus, using different time-temperature modes of the two-stage IR-pyrolysis allows fabricating the Cu-containing PAN films with nanosized particles of copper compounds with different surface morphology. The study of structure and composition of the fabricated films makes it possible to explain their electrical and gas-sensing properties.

The thin films with the resistance values in the range from $4.0 \cdot 10^2$ to $2.7 \cdot 10^{11}$ Ω were fabricated at various IR-annealing temperatures and using various weights of a modifying additive (Fig. 3). As observed from the Fig. 3, the film conductivity was improved significantly by the IR-annealing temperature growth and the increase of copper chloride (II) weight concentration.

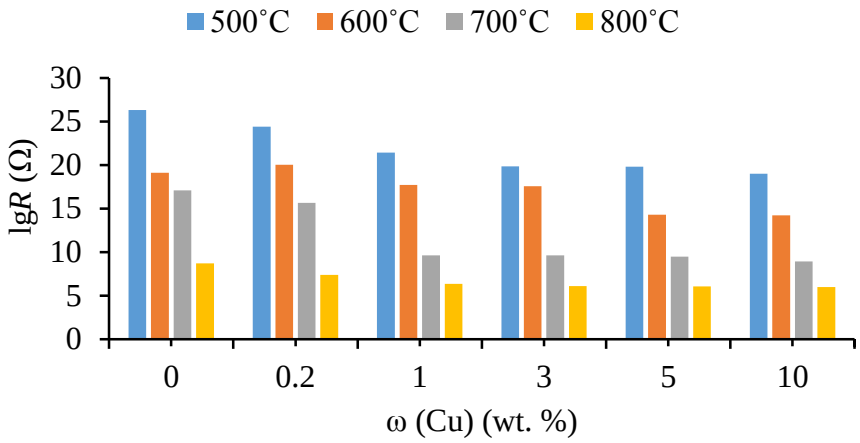

Fig. 3. Histogram, showing the dependence of the film resistance on the weight concentration of a modifying additive and IR-pyrolysis temperature.

According to the results of four-point probe measurements performed on PAN and Cu-containing PAN films, there is the exponential temperature dependence on the films resistance points to the semiconducting nature of the film material [29]. The resistance of the Cu-containing PAN films exponentially decreases with the temperature in the range between room temperature and 70 ºC above that temperature a linear dependence occurs.

The results of the sensing tests of the Cu-containing PAN films revealed their sensitivity to nitrogen dioxide NO_2 in the range of concentration between 36.5 – 255 ppm. The films material behavior is reversible that is the resistance decreases at the adding of NO_2 gas in the air flux, then it restores at fresh air. So, the conductivity of the film increases while adsorbing the gas-oxidizer, as NO_2 is an acceptor of electrons pointing to *p*-type semiconductor

characteristics of film material. In general, the sensitivity of the Cu-containing PAN sensors is affected by technological parameters as well as by the working temperature. The IR-annealing temperatures provide a possibility to manage the gas-sensing properties of the Cu-containing PAN [30].

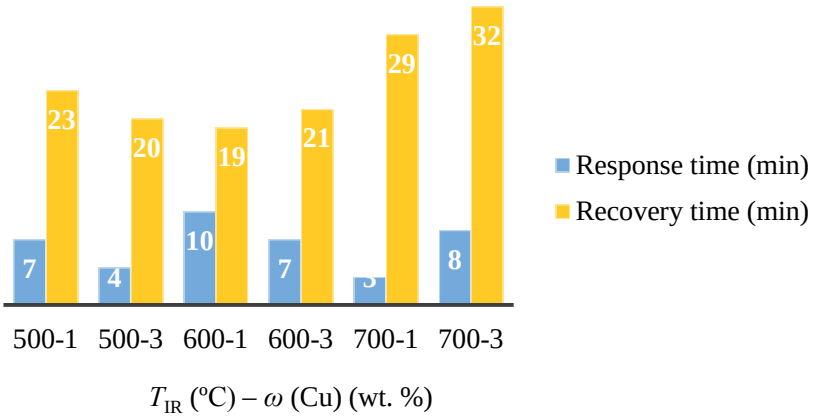

Fig. 4. Response time and recovery time of the Cu-containing PAN sensors *vs* IR-pyrolysis temperature (ºC) and weight concentration of a modifying additive (wt. %), at 20 °C, $c(NO_2)$ = 146 ppm.

The response time and the recovery time of the NO_2 sensors using the Cu-containing PAN nanocomposite films were defined (Fig. 4). The sensors display a relatively rapid response under NO_2 exposure and rather high recovery time: it is extended up to several tens of minutes. The IR-annealing temperatures exert bad influence on the recovery time. To meet the best sensitivity and the fastest response and recovery time requirements a sample, fabricated under 500 ºC from 3 wt. % film-forming solution, was used. The working temperature of the NO_2 sensor with the Cu-containing PAN films sensing layer was determined in the temperatures ranging between 20 °C and 50 °C. The response linearly decreases with the temperature increase in the specified range, the sensitivity of the sensor below 33 ºC was very low (~0.1 r.u.).

The films sensitivity as a function of relative humidity was measured in stationary conditions at 20 ºC. The relative humidity levels are established inside the measurement chamber by fluxing dry air mixed with humidity-saturated air at different ratios [48]. The sensing performances of the films are evaluated by means of electrical measurements, performed while exposing the samples to different relative humidity levels. It was found that within the range of humidity values from 43 % to 90 %, there is no essential change of gas sensitivity.

4. Conclusions

Cu-containing PAN films were fabricated by IR-pyrolysis in ambient argon and their structural and electrical properties were studied. Gas-sensing measurements were performed at low temperature in order to assess the sensing properties of the films for no-heated application. The fabricated films used as a sensing layer for chemo-resistive NO_2 sensor that operates at room temperature. The sensor was found to detect nitrogen dioxide gas down to 36.5 ppm with a reversible and reproducible response.

Acknowledgments. *This work was performed with the financial support of Southern Federal University within project No. VnGr-07/2017-21. The author is greatly thankful for the*

opportunity to fulfill the XPD and spectroscopic investigation to Kabardino-Balkarian State University; AFM investigation to Research and Educational Center of "Nanotechnology" of Southern Federal University; IR-pyrolysis on the installation «FOTON» of the A.I. Topchiev Institute of Petroleum Chemical Synthesis of the Russian Academy of Science.

References

[1] U. Lange, N.V. Roznyatovskaya, V.M. Mirsky // *Analytica Chimica Acta* **614 (**2008) 1.
[2] X. Li, Y. Wang, X. Yang, J. Chen, H. Fu, T. Cheng // *Trends in Anal. Chem.* **39 (**2012) 163.
[3] A. Iwan, D. Sek // *Prog. Polym. Sci*. **33** (2008) 289.
[4] B. Wang, Zh. Chen, X. Zuo, Y. Wu, Ch. He, X. Wang, Z. Li // *Sens. Actuators B* **160** (2011) 1.
[5] G. Han, G. Shi // *Thin Solid Films* **515** (2007) 6986.
[6] T. Fiorido, M. Bendahan, K. Aguir, S. Bernardini, C. Martini, H. Brisset, F. Fages, C. Videlot-Ackermann, J. Ackermann // *Sens. Actuators B* **151** (2010) 77.
[7] A. Singh, S. Samanta, A. Kumar, A.K. Debnath, R. Prasad, P. Veerender, V.Balouria, D.K. Aswal, S.K. Gupta // *Org. Electron* **13** (2012) 2600.
[8] P.P. Sengupta, P. Kar, B. Adhikari // *Thin Solid Films* **517** (2009) 3770.
[9] X. Wang, S. Ji, H. Wang, D. Yan // *Sens. Actuators B* **160** (2011) 115.
[10] S. Javadpour, A. Gharavi, A. Feizpour, A. Khanehzar, F. Panahi // *Sens. Actuators B* **142** (2009) 152.
[11] M.A. Chougule, Sh. Sen, V.B. Patil // *Synth.Met.* **162** (2012) 1598.
[12] S. Srivastava, S. Kumar, Y.K. Vijay // *Int. J. Hydrogen Energy* **37** (2012) 3825.
[13] C. Nandini, B. Sudhapada, S. Palit, M. Mrinal // *J.Polym. Sci. Part B: Polymer Physics* **12** (1995) 1705.
[14] M.A. Geiderikh // *Russ. Chem. Bull.* **14** (1965) 618.
[15] J.J. Ritsko, G. Crecelius, J. Fink // *Phys. Rev. B* **27 (**1983) 2612.
[16] M. Surianarayanan, R. Vijayaraghavan, K.V. Raghavan // *J. Polym. Sci.* **36 (**1998) 2503.
[17] N. Chatterjee, S. Basu, S.K. Palit, M.M. Maiti // *J. Polym. Sci. Part B: Polym. Phys.* **33 (**1995) 1705.
[18] G. Zhanga, H. Mengb, Sh. Jia // *Desalination* **242** (2009) 313.
[19] Q.-Y. Wu, L-S. Wan, Z-K. Xu // *J.Membrane Sci.* **409-410** (2012) 355.
[20] X. He, W. Pu, L. Wang, J. Ren, Ch. Jiang, Ch. Wan // *Electrochim. Acta* **52** (2007) 3651.
[21] X. He, W. Pu, L.Wang, J. Ren, Ch. Jiang, Ch. Wan // *Solid State Ionics* **178** (2007) 833.
[22] S.K. Nataraj, K.S. Yang, T.M. Aminabhavi // *Prog. Polym. Sci.* **37** (2012) 487.
[23] I-H. Chen, Ch.-Ch. Wang, Ch.-Y. Chen // *Carbon* **48** (2010) 604.
[24] M. Jing, Ch. Wang, Q. Wang, Y. Bai, B. Zhu // *Polym. Degrad. Stab.* **92** (2007) 1737.
[25] A.V. Korobeinyk, R.L.D. Whitby, S.V. Mikhalovsky // *Eur.Polym. J.* **48** (2012) 97.
[26] P. Miao, D. Wu, K. Zeng, G. Xu, Ch. Zhao, G. Yang // *Polym. Degrad. Stab.* **95** (2010) 1665.
[27] L.M. Zemtsov, G.P. Karpacheva // *High-molec. Comp*. **6(36)** (1994) 919.
[28] A.N. Korolev, I.S. Al-Hadrami, T.V. Semenistaya, G.P. Karpacheva, L.M. Zemtsov, T.P. Loginova, V.V. Petrov, T.N. Nazarova // *Russian Patent RU 2415158 C2,* 27.03.2011 (In Russian).
[29] I.S. Al-Hadrami, A.N. Korolev, L.M. Zemtsov, G.P. Karpacheva, T.V. Semenistaya // *Mater. Elektr. Tehniki* **1** (2008) 14 (In Russian).
[30] A.N. Korolev, T.V. Semenistaya, I.S. Al-Hadrami, T.N. Nazarova, V.V. Petrov // *Izv. VUZov Elektronika* **1** (2008) 20 (In Russian).
[31] A.A. Dulov, A.A. Slinkin, *Organic Semiconductors* (Nauka, Moscow, 1970) (In Russian).
[32] M.P. Wadekar, C.V. Rode, Y.N. Bendale, K.R. Patil, A.A. Prabhune // *J. Pharm. Biomed. Anal.* **39** (2005) 951.

[33] Y. Matsumura, H.Ishibe // *J. Catal*. **268** (2009) 282.
[34] A. Jagminas, G. Niaura, J. Kuzmarskyte, R. Butkiene // *Appl. Surf. Sci*. **225** (2004) 302.
[35] A.N. Korolev, T.V. Semenistaya, I.S. Al-Hadrami, T.P. Loginova, M. Bruns // *Persp. Mater*. **5** (2010) 52 (In Russian).
[36] http://srdata.nist.gov/xps/
[37] C.D. Wagner, W.M. Riggs, L.E. Davis, J.F. Moulder, G.E. Muilenberg, *Handbook of X-ray Photoelectron Spectroscopy* (Perkin-Elmer Corp., Phys. Electron. Division, Eden Prairie, Minn. 55344, 1979).
[38] G. Beamson, D. Briggs, *High Resolution XPS of Organic Polymers: the Scienta ESCA300 Database* (John Wiley & Sons, Ltd, Chichester, 1992).
[39] V.I. Nefedov, *X-ray Photoelectron Spectroscopy of Chemical Compounds. Handbook.* (Chemistry, Moscow, 1984) (In Russian).
[40] Yu.M. Shulga, V.I. Rubtsov, O.N. Efimov // *Vysokom. Soedin., Seriya A* **36(6)** (1996) 989 (In Russian).
[41] G.A. Shagisultanova, A.V. Shchukarev, T.V. Semenistaya // *Russ. J. Inorg. Chem*. **50(6)** (2005) 912 (In Russian).
[42] L.S. Dake, D.E. King, A.W. Czanderna // *Solid State Sci*. **2** (2000) 781.
[43] R.S. Vieira, M.L.M. Oliveira, E. Guibal, E. Rodríguez-Castellón, M.M. Beppu // *Colloids Surf. A: Physicochem. Eng. Aspects* **374** (2011) 108.
[44] V.W.L. Lim, E.T. Kang, K.G. Neoh // *Synth. Metals* **123** (2001) 107.
[45] D. Zheng, Z. Gao, X. He, F. Zhang, L. Liu // *Appl. Surf. Sci*. **211** (2003) 24.
[46] Z.Mekhalif, F. Sinapi, F. Laffineur, J. Delhalle // *J. Elect. Spectr. and Related Phen*. **121** (2001) 149.
[47] T.V. Semenistaya. In: *Advanced Materials - Manufacturing, Physics, Mechanics and Applications*, *Springer Proceedings in Physics*, ed.by Ivan A. Parinov, Shun-Hsyung Chang, Vitaly Yu. Topolov (Heidelberg, New York, Dordrecht, London: Springer Cham., 2016), Vol. 175, p. 61.
[48] G. Scandurra, A. Arena, C. Ciofi, A. Gambadoro, F. Barreca, G. Saitta, G. Neri // *Sens. Actuators B* **157** (2011) 473.